



Multiple Lines of Ecological Evidence Support Ancient Contact Between the African Wild Dog and the Dhole

Rita Gomes Rocha^{1,2*}, João Gonçalves^{1,2,3}, Pedro Tarroso^{1,2}, Pedro Monterroso^{1,2} and Raquel Godinho^{1,2,4,5*}

¹ InBIO Laboratório Associado, CIBIO—Centro de Investigação em Biodiversidade e Recursos Genéticos, Universidade do Porto, Vairão, Portugal, ² BIOPOLIS Program in Genomics, Biodiversity and Land Planning, Centro de Investigação em Biodiversidade e Recursos Genéticos (CIBIO), Vairão, Portugal, ³ proMetheus—Research Unit in Materials, Energy and Environment for Sustainability, Instituto Politécnico de Viana do Castelo, Viana do Castelo, Portugal, ⁴ Departamento de Biologia, Faculdade de Ciências, Universidade do Porto, Porto, Portugal, ⁵ Department of Zoology, University of Johannesburg, Johannesburg, South Africa

OPEN ACCESS

Edited by:

Hervé Bocherens,
University of Tübingen, Germany

Reviewed by:

Saverio Bartolini Lucenti,
University of Florence, Italy
Ben Sacks,
University of California, Davis,
United States

*Correspondence:

Rita Gomes Rocha
rgrocha@cibio.up.pt
Raquel Godinho
rgodinho@cibio.up.pt

Specialty section:

This article was submitted to
Paleoecology,
a section of the journal
Frontiers in Ecology and Evolution

Received: 28 October 2021

Accepted: 28 April 2022

Published: 19 May 2022

Citation:

Rocha RG, Gonçalves J, Tarroso P, Monterroso P and Godinho R (2022) Multiple Lines of Ecological Evidence Support Ancient Contact Between the African Wild Dog and the Dhole. *Front. Ecol. Evol.* 10:803822. doi: 10.3389/fevo.2022.803822

Genomic tools have greatly enhanced our ability to uncover ancient interspecific gene flow, including cases involving allopatric lineages and/or lineages that have gone extinct. Recently, a genomic analysis revealed the unexpected gene flow between the African wild dog (*Lycaon pictus*) and the dhole (*Cuon alpinus*). The two species have currently highly disjunct and patchy distributions in Africa and Asia, respectively, which are remnants of a much wider past distribution. Yet, no reported evidence of their past contact has ever been documented. By hindcasting the past potential distribution of both species during the Last Glacial Maximum and the Last Interglacial, validating paleoclimatic reconstructions with fossil evidence, quantifying the intersection of their bioclimatic niches, and assessing interspecific compatibility, we investigate the location and favorable conditions for such contact and its ecological validity. We were able to identify the Levant region in Eastern Mediterranean during the Last Interglacial as the most suitable spatio-ecological context for the co-occurrence of the two canids, and to provide evidence of a highly significant overlap of the African wild dog niche with the wider niche of the dhole. These results, combined with ecologic traits, including key compatibility features such as cooperative breeding and hunting, provide consistent support for the potential co-occurrence of both canids. We suggest that the ranges of these canids came into contact multiple times during periods resembling the Last Interglacial, eventually facilitating gene flow between the African wild dog and the dhole in their post-divergence history. Our results are highly supportive of the key role of the Levant region in providing connectivity between African and Eurasian faunas and provide further impetus to combine different tools and approaches in advancing the understanding of species evolutionary histories.

Keywords: fossil evidence, interglacial periods, Levant region, hypervolume analysis, species distribution models, wolf-like canids

INTRODUCTION

The availability of genome-wide data and sophisticated analytical tools have greatly enhanced our ability to decipher the evolutionary trajectory of species, including an unprecedented understanding of interspecific gene flow (Taylor and Larson, 2019). Hybridization has been documented between closely and distantly related species and is now recognized as a driver in the evolutionary history of many taxa (Taylor and Larson, 2019). Mammals have been previously overlooked in this regard (Stebbins, 1959), but recent studies have uncovered unexpected events of ancient hybridization between lineages that are currently allopatric and/or involving lineages that have gone extinct (Koepfli et al., 2015; Cahill et al., 2018; Gopalakrishnan et al., 2018; Palkopoulou et al., 2018; Westbury et al., 2020). Still, these exciting genomic results should be supported by geographic and temporal evidence of coexistence for the species that exchanged genes, and with ecological evidence of niche similarities.

Past contact between species exhibiting signatures of ancient gene flow may be readily validated through evidence of contemporary cohabitation in the fossil record (Varela et al., 2009; Westbury et al., 2020). However, the incompleteness of the fossil record may challenge such an approach, especially in periods or regions with poor paleontological remains, or for species that intrinsically yield less fossil remains as those naturally occurring at low population densities. In these cases, modeling tools allowing to obtain spatiotemporal projections from current to past bioclimatic conditions provide an answer to hindcast past potential contacts between species. Species distribution models (SDMs) are one of the most widely used tools to assess past potential distribution of taxa and have been used to study global change impacts on biodiversity, and to provide key insights into evolutionary questions through paleoclimatic models (Guisan et al., 2013; Leite et al., 2016). SDMs provide a correlative approach to assess species-environment relations using species observations, and/or museum-type records, along with environmental predictor variables (e.g., temperature, rainfall, soil type, vegetation cover) (Elith and Leathwick, 2009). Beyond contemporary spatial overlap, species interbreeding also hinges on a similar ecological niche. A recently applied tool across different fields of ecology and evolution to study species ecological niches is the hypervolume approach (Blonder et al., 2014), which allows interpreting species niches as geometric shapes and quantifies the range of conditions under which a species can survive and reproduce (Blonder, 2018). Spaces occupied by different species can be compared, allowing a quantification of niche differentiation and inference of species coexistence at an ecological level (Carvalho and Cardoso, 2020). Furthermore, anatomic, physiologic, ecologic, and behavioral traits of coexisting species need to be compatible to favor breeding events (Willis, 2013). Although relative body mass, social and reproductive behavior are general key components for interspecific compatibility, hunting strategy, preferred prey and foraging habitats arise as additional important traits when it concerns to terrestrial mammalian carnivores (Vieira and Port, 2007; Bassi et al., 2017).

A recent genomic analysis targeting wolf-like canids revealed extensive admixture between several species pairs, including the unexpected gene flow between the African wild dog (*Lycaon pictus*—hereafter, AWD) and the dhole (*Cuon alpinus*) (Gopalakrishnan et al., 2018). The two species diverged long ago, between ca. 2.5 mya ago (Gopalakrishnan et al., 2018) and ca. 3.91 mya (Chavez et al., 2019), though they exhibit analogous morphological and ecological features (Kamler et al., 2015; Woodroffe and Sillero-Zubiri, 2020). Both are habitat generalists with highly disjunct and patchy distributions in sub-Saharan Africa (Woodroffe and Sillero-Zubiri, 2020) and in the South and East of Asia (Kamler et al., 2015), respectively, which are remnants of a much wider past distribution (Woodroffe et al., 1997; Stiner et al., 2001; Ghezze and Rook, 2014; Makenov, 2018). Gopalakrishnan et al. (2018) have explicitly formulated the speculative hypothesis that both species could have admixed in North Africa, owing to the fossil evidence of the dhole as far west as Europe during the Pleistocene (Ghezze and Rook, 2014). However, no evidence supporting their past contact or exploring interspecific compatibility has ever been documented.

To explicitly investigate the possible past contact between the AWD and the dhole, we have: (i) Assessed the current and the past potential distribution areas validating our approach with the available fossil evidence, (ii) tested the overlap between species bioclimatic niches, and (iii) assessed their relatedness in ecological, behavioral, and trophic traits. Using this integrative approach, we aim to gain insights on the evolutionary history of wolf-like canids and to explore complementary tools to test past contact between species.

METHODS

Current Species Occurrence Data

Geographic records of each species presence were obtained from the online database GBIF¹ and reviews of the species distribution with available datasets (Johnsingh, 2009; Makenov, 2018). Geographic records from GBIF were matched with the species distribution to detect and remove possible inaccurate records from the preliminary data sets.

We performed a search in the Web of ScienceSM using the species name as a single keyword to retrieve geographic records of the species from available literature in a variety of study fields, including ecology, conservation, population genetics, and phylogeography. Scientific articles were checked for either GPS coordinates or maps of the sampling localities. Geographic coordinates were directly annotated in our database, whereas data available only in maps were obtained through hand-digitization and spatial georeferencing in QGIS (QGIS Development Team, 2020). Georeferencing was performed using 1st–3rd order polynomials. Control points were progressively inserted and/or removed to lower the positional error to a minimum. If the error was considered unacceptable (depending on each case), the map was discarded and records were not added.

¹<https://www.gbif.org>

Because the current distribution of both AWD and dhole is highly reduced (Kamler et al., 2015; Woodroffe and Sillero-Zubiri, 2020), their historical distribution ranges are essential to account for the full climatic niches (Martínez-Freiría et al., 2016). For that, we also searched for historical records, such as those included in specialist group reports and past distribution reviews (Woodroffe et al., 1997; Makenov, 2018). Geographic records of both species spanned from the eighteenth century to the present.

Records from different sources were later combined and harmonized into a coherent database. In addition, prior to modeling routines, we performed a two-step filtering process by (1) removing presence duplicates per pixel of environmental variables, and (2) applying an environmental filtering of all records² following Varela et al. (2014) to reduce spatial autocorrelation and clustering issues in the data. These procedures have been found to improve models across several scales (Castellanos et al., 2019).

Fossil Occurrence Data

Fossil records of each species were obtained from the Paleobiology Database³ and by searching the Web of ScienceSM using the species name and “fossil” as keywords. Fossil records of the dhole throughout Europe were made available by Elena Ghezzeo (Ghezzeo and Rook, 2014). This database was updated with recent studies of both species (Faith, 2013; Liu et al., 2015; Shao et al., 2015; Collins, 2016; Volmer et al., 2019; Liang et al., 2020; Mecozzi et al., 2020; Marciszak et al., 2021). Due to the intricate taxonomy of the dhole (Volmer et al., 2019), we only considered fossil records identified at species level, including all subspecies of *C. alpinus*, such as the southern dhole *C. a. javanicus* (Volmer et al., 2019). The only exception was *Cuon priscus*, which is either referred to as a different species (Volmer et al., 2019) or as a subspecies of *C. alpinus* (Marciszak et al., 2021). Due to this taxonomic uncertainty, fossil records of *C. priscus* were not considered in this study. Nonetheless, the range of fossils from this species is fully covered by the fossil dataset for *C. alpinus*. Hand-digitization and spatial georeferencing of fossil records from the literature were performed as described above.

In addition to the fossil location, fossil age estimates were also recorded when available (**Supplementary Table 1**). Fossils without age estimates were excluded. To investigate the presence of the AWD and the dhole during glacial and interglacial periods, fossils were classified into five temporal categories: (i) Last Glacial, for fossils dated to the Last Glacial Period between Marine Isotope Stage 4 and Marine Isotope Stage 2 [MIS4–MIS2: *ca* 70–15 kya (Helmens, 2014)]; (ii) Last Interglacial, for fossils dated to the Last Interglacial *sensu lato* at Marine Isotope Stage 5 [MIS5: *ca* 130–70 kya (Helmens, 2014)]; (iii) other glacial, for fossils dated to Marine Isotope Stage 6 [MIS6: *ca* 185–135 kya (Roucoux et al., 2011)]; (iv) other interglacial, for fossils dated to other interglacial periods, including the Holocene (<11.7 kya) and the Marine Isotope Stage 7 [MIS7: *ca* 246–195 kya (Tzedakis et al., 2004; Geyh and Thiedig, 2008)]; and (v)

Glacial and Interglacial, for fossils dated to very wide periods encompassing multiple cycles of glacial and interglacial periods.

Bioclimatic Predictors

Bioclimatic variables (derived from monthly temperature and rainfall data to generate more ecologically meaningful variables) were used to portray the suitable conditions in temperature and precipitation of each species niche. These climatic data for current historical conditions (1979–2013) were based on the CHELSA v-1.2b climate dataset and made available from PaleoClim dataset (Brown et al., 2018) at a spatial resolution of 5 arc-minute, ~9 km at the equator. CHELSA is based on a quasi-mechanistical statistical downscaling method of reanalysis and the ERA-Interim global circulation model (Karger et al., 2017).

Paleoclimatic reconstructions for past periods included the Pleistocene Last Glacial Maximum [LGM; ~21 kya; based on an implementation of the CHELSA algorithm on PMIP3 data in Karger et al. (2017)] and the Last Interglacial (LIG; 130 kya; based on Otto-Bliesner et al., 2006). Both LGM and LIG climate data were obtained from the PaleoClim dataset (Brown et al., 2018) with a spatial resolution of 5 arc-minute.

The assessment of pairwise correlations for the 19 bioclimatic variables was performed over a large area defined by a 10° buffer around each presence. Pearson correlations were calculated for all pairwise combinations of variables using the raster package v. 3.1.5 (Hijmans and van Etten, 2020) in R v. 4.0.2 (R Core Team, 2020). The complement of the absolute correlation score was used in hierarchical cluster analysis with single linkage to choose the least correlated variables. To reduce the multicollinearity and improve parsimony, we calculated the variance inflation factor (VIF) for the final set of variables using the car package v. 3.0 (Fox and Weisberg, 2019) in R.

Model Development, Evaluation, Multi-Algorithm Ensembling and Filtering

Species Distribution Models were developed in R v. 4.0.2 using the biomod2 package (Thuiller et al., 2009). This package implements a multi-model ensemble forecasting approach that combines several existing statistical and machine-learning-based algorithms, enabling to assess and prevent a range of methodological uncertainties in each individual modeling algorithm and the examination of species-environment relationships. Models were fitted using nine modeling techniques currently available in biomod2: GLM (Generalized Linear Models); GBM (Generalized Boosted Models); GAM (Generalized Additive Models); CTA (Classification Tree Analysis); ANN (Artificial Neural Networks); FDA (Flexible Discriminant Analysis); MARS (Multivariate Adaptive Regression Splines); RF (Random Forests); MAXENT.Phillips2 (Maximum Entropy Model). Default parameters were employed, except the smoothing degree term in GAM, which was set to $k = 4$ to avoid over-fitting issues (Guisan et al., 2002), and the number of boosting trees in GBM, which was set to $n.trees = 2,000$.

²<https://github.com/SaraVarela/envSample>

³<https://paleobiodb.org/>

Given that only presence data was available for the selected species, we established a total of ten sets of randomly generated global pseudo-absences (PA), each set with an equal number of pseudo-absences as the number of presence records, as suggested by Barbet-Massin et al. (2012) for classification techniques which dominate biomod2. By using ten sets of pseudo-absences we forced models to learn species ecological responses to climate with much greater variability, resulting in an effect similar to increasing the number of pseudo-absences per set. Since no previous information was assumed about species prevalence (p), model weights were adjusted to set $p = 0.5$ (biomod2 default) thus giving similar weight to presences and pseudo-absences. Although different algorithms are affected differently by the sample prevalence, by using the same number of pseudo-absences as presences we maintain the prevalence in each model, allowing models to calibrate with balanced conditions.

Holdout cross-validation (HOCV) was employed to evaluate the models with 80% of the input records used for model fitting and 20% for model evaluation at each round. A total of ten cross-validation rounds were performed for model evaluation. A final round including all species presence records was also performed. For assessing model performance, we calculated for the test sets the Area Under the Curve (AUC; varying from 0 to 1, with values closer to one signaling better models), the True-skill Statistic (TSS; varying from -1 to 1 , with values closer to one signaling better models), and the Sensitivity (or true positive rate) and the Specificity (true negative rate) values (both from 0 to 100% with values closer to 100% signaling better predictions from models). We also estimated the Sørensen and Jaccard metrics following Leroy et al. (2018).

Given that 990 partial models were generated per species (i.e., generated by each combination of modeling algorithm, pseudo-absence set and evaluation round) it was necessary to select a subset of these for the final projective ensemble. This selection was performed in two main steps ensuring that the best performing algorithms and data subsets used for model calibration were selected. First, the six best-performing modeling techniques (out of nine) were ranked and selected according to the median TSS value. Second, we selected the top 20% percentile best-models, also considering the TSS distribution, for each of the previously six selected algorithms. Based on these top-performing models, an ensemble of the spatial projections using the average was calculated for the 198 models previously selected ($n = 6$ algorithms \times 33 combinations of PA sets and HOCV/full sets). The classification of model prediction into a binary outcome of presence/absence was performed using the probabilistic threshold value maximizing the TSS statistic.

Finally, ensemble consensus model projections obtained for each period/species were filtered to increase their congruence with known present and past species records. In this process, we filtered out all model projected suitable pixels lying outside an expanded minimum convex polygon comprised by all known current and fossil records (with a buffer distance of 1,270 km, i.e., the minimum distance between AWD and dhole fossil records in the Levant region).

To assess the spatial overlap between fossil data and model projections for the two past periods, we calculated the percentage

of records that have climatically suitable areas considering two distance buffers of 100 and 250 km around each fossil point. R packages *sf* (Pebesma, 2018) and *raster* (Hijmans and van Etten, 2020) were employed in these calculations.

Hypervolume Analysis

The intersection of the niches of both species was quantified following the hypervolume approach (Blonder et al., 2014). Here the collected environmental data at each presence location for each species is compared after the estimation of the volume of the niche on the n -dimensional space. This approach allows for comparisons between niche's hypervolumes, such as the unique fractions of each niche, intersection dimension and union.

We used the previously selected climate variables for hypervolume quantification. Due to the very different sample sizes of each species ($n_{Lycanopictus} = 1,284$; $n_{Cuonalpinus} = 525$), we followed an iterative approach with balanced resampled data sets. On each iteration, we randomly chose 250 presences of each species to build and compare the hypervolumes and run sufficient iterations to assure that every presence record was used at least once. Niche volumes were scaled with the volume of the union of both niches and, thus, presented in percentages in relation to the maximum environmental area covered by both species. Additional to niche volume quantification we calculated the overlap index (OI), which is equivalent to the Sorenson distance normalized by the smallest niche volume and has the ability to detect overlap even in the case of asymmetrical niche sizes (Simó-Riudalbas et al., 2018). To test the OI, we followed a niche equivalency test (Warren et al., 2008), where we randomly sampled 250 samples from the pooled iteration data set for each species under the null hypothesis that niches are identical. We used 100 replicates in each iteration to test the significance of OI.

Interspecific Compatibility Assessment

Species-level morphological, habitat and population traits, as well as reproductive, social and feeding behavior were compiled for the dhole and the AWD from specialized literature. These traits included mean body mass, dental morphology, generation length, litter size, breeding strategy, pack size, activity, feeding strategy, habitat, home range, and population density.

In addition, trophic niches of the dhole and the AWD were reconstructed based on the recently published CarniDIET (v1.0) database (Middleton et al., 2021). We assembled all prey species in dhole and AWD samples (scats, stomachs or kills) with a mean frequency of occurrence (FO) larger than 5% to exclude occasionally consumed items. We further filtered prey species to exclude domestic animals. Each prey was then characterized with regard to its taxonomic position and body mass using the PHYLACINE 1.2.1 database (Faurby et al., 2018, 2020), to its social group size using the PanTHERIA database (Jones et al., 2009) and to its habitat preferences using IUCN's red list assessments (for the full list of prey species, please see **Supplementary Tables 2, 3**). Habitat classes were considered at its most basal level—forest, savanna, shrubland, grassland, wetland, rocky area, and desert—allowing for a comparison of habitat preferences concerning fundamental vegetation structure, and its importance was considered as: (i) Crucial, if the habitat

is important for the survival of the species, either because it has an absolute requirement for the habitat at some point in its lifecycle or because it is a primary habitat within which the species or most individuals occur; (ii) Suitable, if the species occurs in the habitat regularly or frequently; or (iii) Marginal, if the species occurs in the habitat only irregularly or infrequently, or only a small proportion of individuals are found in the habitat⁴.

We further matched this database with the Elton Trait 1.0 database (Wilman et al., 2014), to obtain Eltonian niches of diet, foraging strata and diel activity patterns, allowing to categorize the functional groups of prey consumed by both the dhole and the AWD. Based on the full spectrum of prey species in the CarniDIET database ($n = 810$), prey body masses (BM) were clustered into seven discrete categories using the Jenks natural breaks classification method with the BAMMTools package for R (Rabosky et al., 2014). This method minimizes the variance within categories while maximizing the variance between categories. Defined classes were as “Very small” ($BM < 11$ kg), “Small” ($11 \text{ kg} \leq BM < 38$ kg), “Intermediate” ($38 \text{ kg} \leq BM < 82$ kg), “Intermediate large” ($82 \text{ kg} \leq BM < 143$ kg), “Large” ($143 \text{ kg} \leq BM < 250$ kg) and “Extremely large” ($BM \geq 250$ kg).

RESULTS

The variable selection procedure delimited a final set of five bioclimatic variables that best represent the suitable conditions in temperature and precipitation of each species' niche. These included the temperature-related BIO_06 [Minimum Temperature of Coldest Month ($^{\circ}\text{C} \times 10$), VIF = 1.6] and four precipitation variables, namely BIO_12 [Annual Precipitation (mm/year), VIF = 5.1], BIO_14 [Precipitation of Driest Month (mm/month), VIF = 1.8], BIO_18 [Precipitation of Warmest Quarter (mm/quarter) VIF = 2.8] and BIO_19 [Precipitation of Coldest Quarter (mm/quarter), VIF = 2.2].

The predictive performance of the average ensemble models resulted in robust statistics for both species, though consistently illustrating higher or similar values for the AWD (TSS = 0.86, AUC = 0.9, Jaccard similarity = 0.85, Sørensen similarity = 0.92) than for the dhole (TSS = 0.73, AUC = 0.94, Jaccard similarity = 0.76, Sørensen similarity = 0.86; **Supplementary Tables 4, 5**). No modeling algorithm was consistently worse than any other, with both the ensemble and Random Forest (RF) having on average the best fit for both species (**Supplementary Table 5**).

The suitable geographic area available for both the AWD and the dhole suffered an extensive decrease from LIG (**Figure 1**) to LGM (**Supplementary Figure 1**), and then slightly increased toward the present, mainly for the dhole (**Supplementary Figure 2**). During the LIG, the SDMs projected suitable areas for the AWD in most of continental Africa and the Middle East, and for the dhole in the South and East Asia, Ural Region, Southern and Central Europe, and the Caucasus (**Figure 1**).

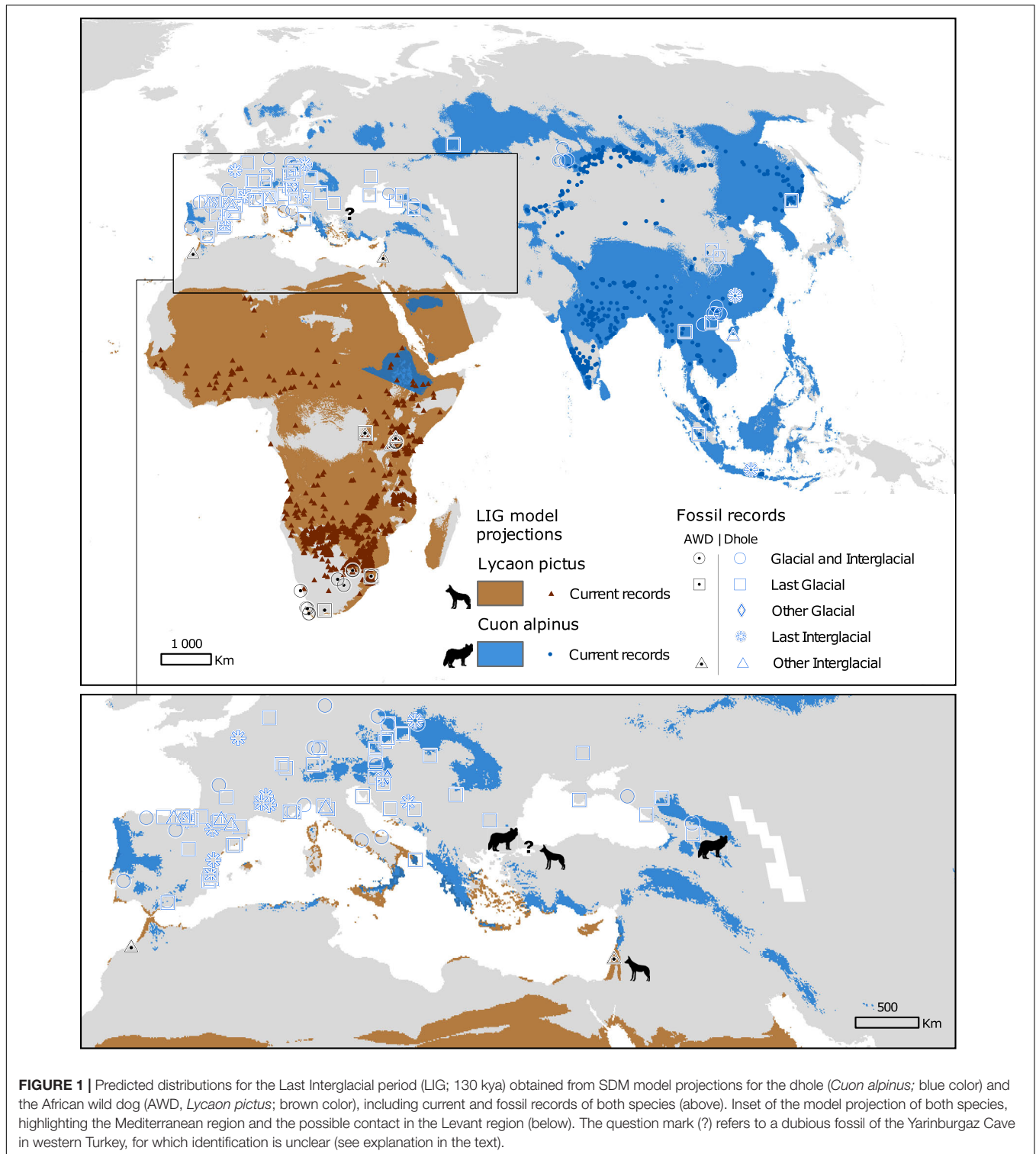
Notably, projected distributions of both species overlap during LIG in several areas in the Northern and Eastern coast of the Mediterranean, namely the Levant Region, southern Turkey, Greece and Italy, and in the Iberian Peninsula, including the Strait of Gibraltar region both in Europe and Africa. Projected suitable areas for the dhole in Scandinavia and continental Africa resulted from favorable climatic conditions in these regions, but do not overlap with any historical or current evidence of presence for this species (**Figure 1**), therefore were not considered in further inferences.

Fossil records during the Last Glacial Period and the Last Interglacial, and also fossil records dated to very wide periods encompassing multiple cycles of glacials and interglacials, appear within the projected suitable areas for the AWD and the dhole (**Figure 1** and **Supplementary Table 1**). No fossil evidence was recorded for the dhole in the African continent, while the single AWD fossil record outside Africa was found in the Levant region (Hayonim Cave, Israel) and dates from an interglacial period at the MIS7 or at the interglacial intervals of the MIS6 (**Figure 1** and **Supplementary Table 1**). Notwithstanding, several fossil records appear outside the projected suitable areas, particularly in South Africa for the AWD and in the east of the Iberian Peninsula and central Europe for the dhole, suggesting that the current distribution data do not represent the entire climatic niche of both species (Varela et al., 2009). The spatial overlap between fossil data and model projections during the LGM is higher for the AWD than the dhole (87.5–100% vs. 35.7–85.7%, respectively, **Supplementary Table 6**). Whereas during the LIG, the spatial overlap is similar for both species (76.9% vs. 38.5–84.3%, respectively, **Supplementary Table 6**).

Hypervolumes of each species inferred using a 5-dimensional analysis were built and compared for 37 iterations to assure that all presence records were used at least once in the process. The niche of the dhole emerged as substantially larger than the niche of the AWD, comprising $99.99 \pm 0.01\%$ and $0.35 \pm 0.13\%$ of the niches' union, respectively (**Figure 2**). The intersection of niches represented $0.34 \pm 0.12\%$ of the union volume, indicating that the niche of the dhole contains most of the smaller niche of the AWD (**Figure 2**). This was further supported by the high value observed for the overlap index ($OI = 0.97 \pm 0.02\%$), significantly higher than random ($\alpha = 0.05$) in 36 of the 37 iterations.

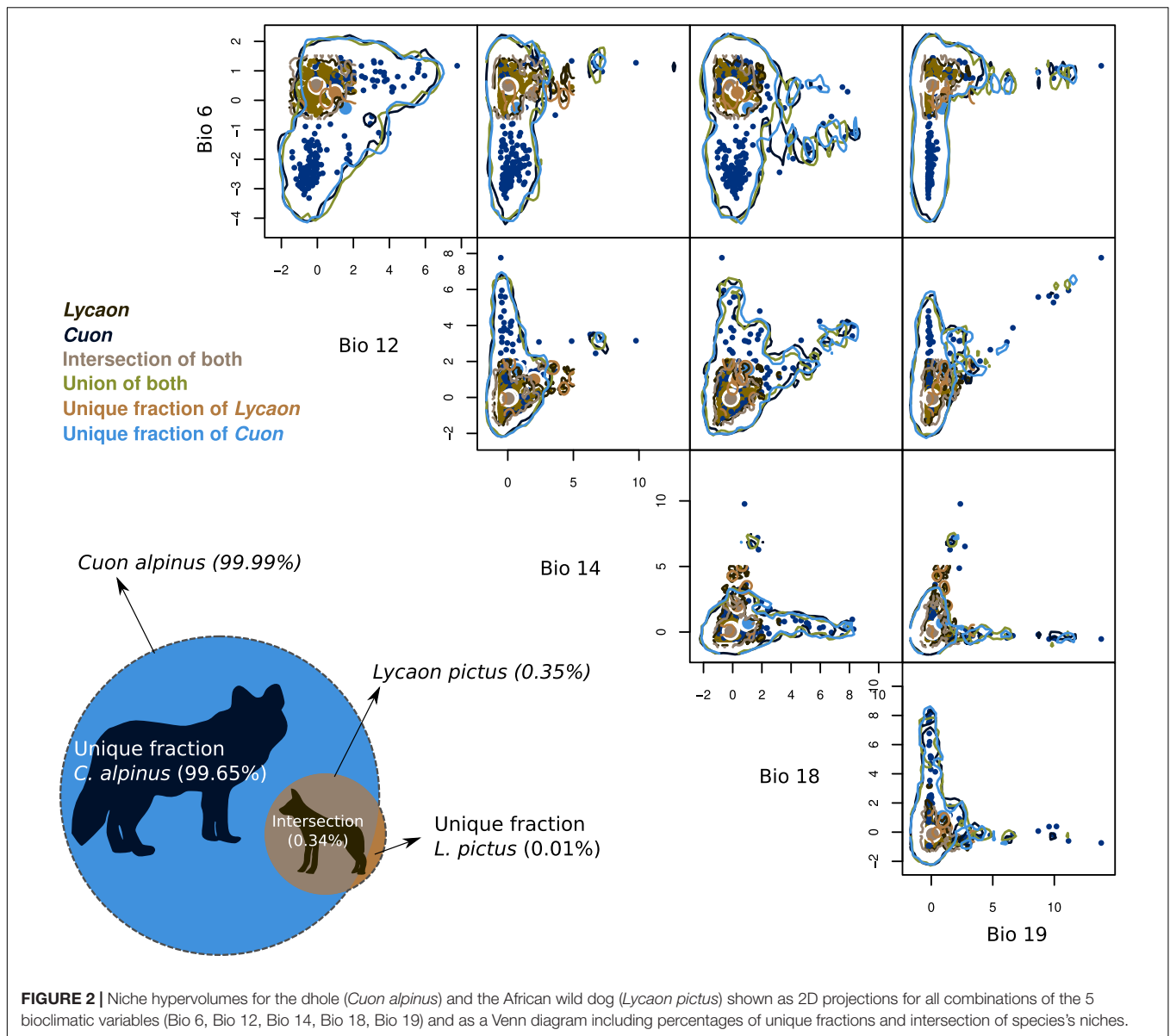
Despite the dhole's smaller size, we found high levels of similarity between the two canids in most analyzed traits (**Table 1**). Both the AWD and the dhole inhabit a wide variety of habitats, from forests to grassland areas, although the AWD is mostly restricted to dry environments (Kamler et al., 2015; Woodroffe and Sillero-Zubiri, 2020). Social, reproductive and feeding behaviors of the two canids are highly similar, including equivalent key compatibility traits such as cooperative breeding and hunting (**Table 1**). Both canids prey on very small to extremely large prey species and have an equivalent number of regularly consumed items ($n_{Lycanopictus} = 14$ vs. $n_{Cuonalpinus} = 12$) (**Supplementary Figure 3**). Dhole' prey include species of the families Bovidae ($n = 4$), Cervidae ($n = 4$), Leporidae ($n = 1$), Mustelidae ($n = 1$), Ochotonidae ($n = 1$) and Suidae ($n = 1$), while AWD prey regularly on species of Bovidae ($n = 13$)

⁴<https://www.iucnredlist.org/resources/habitat-classification-scheme>



and Suidae ($n = 1$) (Supplementary Table 2). Despite the AWD tend to consume slightly heavier species, we found no differences in body mass distributions of prey ($t = 0.42$, $df = 13.017$, $p\text{-value} = 0.6775$). AWDs and dholes find prey across a variety of habitats, although preferred species may

be particularly available in open areas such as grasslands and savannas (Supplementary Figure 3 and Supplementary Table 3). Additionally, regularly consumed prey are active across the diel cycle for both species (Supplementary Figure 3 and Supplementary Table 2).



DISCUSSION

We found consistent support for range dynamics of the AWD and the dhole, and their potential past range overlap during the environmental conditions of the LIG. The projected distributions of both species during this period overlap in the Levant Region, as well as in other Mediterranean regions, including the Strait of Gibraltar region both in Europe and Africa (Figure 1).

To assess whether transferability to the past could have been constrained by limited current data (Varela et al., 2009), we validated our models using fossil evidence within the projected potential distributions (Nogués-Bravo, 2009). This inference strengthened the hypothesis of potential past contact between the two species by supporting the presence of the AWD in the Levant region (Hayonim Cave, Israel) during the interglacial period of the MIS7 or at the interglacial intervals of the MIS6

(Stiner et al., 2001; Ayalon et al., 2002), whilst revealing the nearest presence of the dhole (ca. 1,000 km north) in the Caucasus (Kudaro 3 Cave, Georgia) over a concurrent period (Baryshnikov, 1996). Noteworthy is a possible concomitant occurrence of AWD and dhole at the Yarinburgaz Cave in western Turkey (Stiner et al., 1996, 2001). However, whether these records represent two distinct fossils or a misidentification of the same fossil remains unclear. Fossil identification of these canids solely based on morphology is very challenging owing to some overlap in dimensions (Taron et al., 2021). We claim that the robust prediction of concordant suitable geographic areas with favorable bioclimatic conditions, together with the incomplete nature of the fossil record, particularly for species that live at low population densities as the AWD (Stiner et al., 2001; Woodroffe and Sillero-Zubiri, 2020), and the ability for long distance movements by large carnivores, suggest the potential

TABLE 1 | Morphological and ecological traits of the dhole (*Cuon alpinus*) and the African wild dog (*Lycaon pictus*), and the literature source for each trait.

| Traits | <i>Cuon alpinus</i> | <i>Lycaon pictus</i> | Source |
|--------------------------------------|---|---|---|
| Morphological traits | | | |
| Mean body mass | 14 kg | 22 kg | Wilman et al., 2014 |
| Dental morphology | Specialized dental morphology for obligate hypercarnivory | Specialized dental morphology for obligate hypercarnivory | Kamler et al., 2015; Chavez et al., 2019 |
| Reproductive behavior | | | |
| Generation length | 5 Years | 5 Years | Kamler et al., 2015; Woodroffe and Sillero-Zubiri, 2020 |
| Litter size | 5–10 On average, but up to 12 pups | 10–11 On average, but up to 21 pups | Woodroffe et al., 1997; Kamler et al., 2015 |
| Breeding strategy | Obligate cooperative breeders | Obligate cooperative breeders | Woodroffe et al., 1997; Kamler et al., 2015 |
| Social behavior | | | |
| Pack size | 5–25 | 2–27 | Woodroffe et al., 1997; Kamler et al., 2015 |
| Feeding behavior | | | |
| Activity | Diurnal and crepuscular | Diurnal and crepuscular | Wilman et al., 2014 |
| Feeding strategy | Hypercarnivory, cooperative hunting | Hypercarnivory, cooperative hunting | Woodroffe et al., 1997; Kamler et al., 2015 |
| Habitat and population traits | | | |
| Habitat | Grassland, Shrubland, Forest | Grassland, Shrubland, Savanna, Forest, Desert | Kamler et al., 2015; Woodroffe and Sillero-Zubiri, 2020 |
| Home range | 23–199 km ² | 50–2,000 km ² | Woodroffe et al., 1997; Kamler et al., 2015 |
| Population density | 6.6–30 adults/100 km ² | 0.67–4.6 adults/100 km ² | Woodroffe et al., 1997; Kamler et al., 2015 |

co-occurrence of the AWD and the dhole in the Levant region during an interglacial period. This finding is entirely concordant with the key role of the Levant region in connecting African and Eurasian faunas (Belmaker, 2010; Martínez-Navarro, 2010). In particular, the narrow coastal strip in this region known as the Levantine Corridor, where the AWD fossil was detected (Stiner et al., 2001), has been considered the major route between the two continents, where both climatic and ecological conditions have promoted the dispersal, contact and, in some cases, admixture between African and Eurasian counterparts (Belmaker, 2010; Martínez-Navarro, 2010; Koepfli et al., 2015). The presence of the AWD outside Africa, particularly in the Levant region, would conform to a potential reduced competition with local ecologically equivalent taxa, as previously reported for other African carnivores (Belmaker, 2010). Notwithstanding, the competition with the dhole or other similar canids (e.g., the gray wolf *Canis lupus*) more adapted to the Northern Hemisphere conditions, could have limited further expansion of the AWD into Eurasia (Stiner et al., 2001).

Other Mediterranean regions in southern Europe could also be suggested as potential contact areas for the AWD and the dhole, but the large geographical distances between known fossils hampers further inferences. Although fossil evidence supports the presence of dhole across southern Europe mostly until the Last Glacial Maximum, and as late as the beginning of the Holocene in the Iberian Peninsula (Ripoll et al., 2010; Ghezzeo and

Rook, 2014; Puzachenko and Markova, 2019), no other fossil of AWD was found outside Africa (Stiner et al., 2001).

Beyond the spatial overlap of the two canids, the emergence of interspecific gene flow would also depend upon the ecological niche of each species and interspecific compatibility. By investigating the abiotic-related factors of the two species' niches and quantifying their intersection, we have found a substantially larger ecological niche for the dhole, known to be the more generalist of the pair (Kamler et al., 2015; Woodroffe and Sillero-Zubiri, 2020), remarkably comprising most of the AWD niche with a highly significant overlap index. Furthermore, we found high levels of similarity between the two canids in most of the analyzed eco-behavioral traits, including key compatibility features such as cooperative breeding and hunting. From a feeding ecology and prey selection perspective, both canids tend to exhibit an eclectic hypercarnivore diet (Kamler et al., 2015; Woodroffe and Sillero-Zubiri, 2020). We found no differences in the number of regularly consumed prey nor in the prey body mass, and both species use a variety of habitats across the diel cycle to find their prey. Jointly, these results provide support for the potential co-occurrence and ecological compatibility of these two canids, eventually providing the opportunity for gene flow during a period of favorable conditions in their post-divergence history. The signature of gene flow observed by Gopalakrishnan et al. (2018) could result from hybridization between other ancient and concurrent species of *Cuon* and *Lycaon*, though fossil

ages from extinct species of these genera fairly overlap (Marciszak et al., 2021). This was not explored by genomic approaches.

CONCLUSION

By performing paleoclimatic range reconstructions, testing the bioclimatic niche overlap and assessing interspecific compatibility for the AWD and the dhole, we have supported the hypothesis of ancient contact for these two large canids. Although our modeling approach focused only the late Pleistocene, it is likely that the ranges of these species came into contact multiple times during similar conditions to those provided by the LIG. Therefore, gene flow between the AWD and the dhole revealed by genomic approaches could have been possible during favorable periods in their post-divergence history. Our results provide further impetus to combine different tools and approaches to advance the understanding of species evolutionary histories, particularly those with such intricate history as wolf-like canids.

DATA AVAILABILITY STATEMENT

The original contributions presented in the study are included in the article/**Supplementary Material**, further inquiries can be directed to the corresponding author/s.

AUTHOR CONTRIBUTIONS

RR and RG conceived the idea. RR collected the data. JG, PT, and PM performed the analysis. All authors contributed to writing the manuscript.

REFERENCES

- Ayalon, A., Bar-Matthews, M., and Kaufman, A. (2002). Climatic conditions during marine oxygen isotope stage 6 in the eastern Mediterranean region from the isotopic composition of speleothems of Soreq Cave, Israel. *Geology* 30, 303–306. doi: 10.1130/0091-76132002030<0303:CCDMOI<2.0.CO;2
- Barbet-Massin, M., Jiguet, F., Albert, C. H., and Thuiller, W. (2012). Selecting pseudo-absences for species distribution models: how, where and how many? *Methods Ecol. Evol.* 3, 327–338. doi: 10.1111/j.2041-210X.2011.00172.x
- Baryshnikov, G. F. (1996). The dhole, *Cuon alpinus* (Carnivora, Canidae), from the Upper Pleistocene of the Caucasus. *Acta Zool. Cracov.* 39, 67–73.
- Bassi, E., Canu, A., Firmo, I., Mattioli, L., Scandura, M., and Apollonio, M. (2017). Trophic overlap between wolves and free-ranging wolf × dog hybrids in the Apennine Mountains, Italy. *Glob. Ecol. Conserv.* 9, 39–49. doi: 10.1016/j.gecco.2016.11.002
- Belmaker, M. (2010). “Early Pleistocene Faunal Connections Between Africa and Eurasia: An Ecological Perspective,” in *Out Of Africa I: The First Hominin Colonization Of Eurasia*, eds J. G. Fleagle, J. J. Shea, F. E. Grine, A. L. Baden, and R. E. Leakey (Dordrecht: Springer), 183–205. doi: 10.1007/978-90-481-9036-2_12
- Blonder, B. (2018). Hypervolume concepts in niche- and trait-based ecology. *Ecography* 41, 1441–1455. doi: 10.1111/ecog.03187
- Blonder, B., Lamanna, C., Violle, C., and Enquist, B. J. (2014). The n-dimensional hypervolume. *Glob. Ecol. Biogeogr.* 23, 595–609. doi: 10.1111/geb.12146

FUNDING

RR, JG, PT, and RG were supported by the research contracts [CEECIND/01087/2018, CEECIND/02331/2017/CP1423/CT012, DL57/2016/CP1440/CT0008, and DL57/2016/CP1440/CT(SFRH/BPD/88496/2012), respectively] from the Portuguese Foundation for Science and Technology (FCT). PM was supported by the UID/BIA/50027/2021 with funding from FCT/MCTES through national funds. Work co-funded by the project NORTE-01-0246-FEDER-000063, supported by the Norte Portugal Regional Operational Programme (NORTE2020), under the PORTUGAL 2020 Partnership Agreement, through the European Regional Development Fund (ERDF). JG developed this work within the scope of the project proMetheus (Research Unit on Materials, Energy and Environment for Sustainability, FCT Ref. UID/05975/2020).

ACKNOWLEDGMENTS

We thank Elena Ghezzi for kindly sharing the fossil records of the dhole throughout Europe. Species silhouettes used in the figures of this manuscript were obtained from PhyloPic (phylopic.org). Credits of the dhole silhouette are due to Renata F. Martins (<https://creativecommons.org/licenses/by-nc/3.0/>). We thank the reviewers for valuable comments on the previous version of this manuscript.

SUPPLEMENTARY MATERIAL

The Supplementary Material for this article can be found online at: <https://www.frontiersin.org/articles/10.3389/fevo.2022.803822/full#supplementary-material>

- Brown, J. L., Hill, D. J., Dolan, A. M., Carnaval, A. C., and Haywood, A. M. (2018). PaleoClim, high spatial resolution paleoclimate surfaces for global land areas. *Sci. Data* 5:180254. doi: 10.1038/sdata.2018.254
- Cahill, J. A., Heintzman, P. D., Harris, K., Teasdale, M. D., Kapp, J., Soares, A. E. R., et al. (2018). Genomic Evidence of Widespread Admixture from Polar Bears into Brown Bears during the Last Ice Age. *Mol. Biol. Evol.* 35, 1120–1129. doi: 10.1093/molbev/msy018
- Carvalho, J. C., and Cardoso, P. (2020). Decomposing the Causes for Niche Differentiation Between Species Using Hypervolumes. *Front. Ecol. Evol.* 8:243. doi: 10.3389/fevo.2020.00243
- Castellanos, A. A., Huntley, J. W., Voelker, G., and Lawing, A. M. (2019). Environmental filtering improves ecological niche models across multiple scales. *Methods Ecol. Evol.* 10, 481–492. doi: 10.1111/2041-210X.13142
- Chavez, D. E., Gronau, I., Hains, T., Kliver, S., Koepfli, K. P., and Wayne, R. K. (2019). Comparative genomics provides new insights into the remarkable adaptations of the African wild dog (*Lycaon pictus*). *Sci. Rep.* 9:8329. doi: 10.1038/s41598-019-44772-5
- Collins, B. (2016). Foraging strategies during the final Middle Stone Age occupation at Sibudu Cave, South Africa. *J. Archaeol. Sci. Rep.* 5, 61–70. doi: 10.1016/j.jasrep.2015.10.035
- Elith, J., and Leathwick, J. R. (2009). Species Distribution Models: ecological Explanation and Prediction Across Space and Time. *Annu. Rev. Ecol. Evol. Syst.* 40, 677–697. doi: 10.1146/annurev.ecolsys.110308.120159

- Faith, J. T. (2013). Taphonomic and paleoecological change in the large mammal sequence from Boomplaas Cave, western Cape, South Africa. *J. Hum. Evol.* 65, 715–730. doi: 10.1016/j.jhevol.2013.09.001
- Faurby, S., Davis, M., Pedersen, R. Ø., Schowaneck, S. D., Antonelli, A., and Svenning, J. C. (2018). PHYLACINE 1.2: the Phylogenetic Atlas of Mammal Macroecology. *Ecology* 99:2626. doi: 10.1002/ecy.2443
- Faurby, S., Pedersen, R. Ø., Davis, M., Schowaneck, S. D., Jarvie, S., Antonelli, A., et al. (2020). MegaPast2Future/PHYLACINE_1.2: PHYLACINE Version 1.2.1 (v1.2.1). Zenodo. doi: 10.5281/zenodo.3690867
- Fox, J., and Weisberg, S. (2019). *An R Companion To Applied Regression*. Third. Thousand Oaks CA: Sage.
- Geyh, M. A., and Thiedig, F. (2008). The Middle Pleistocene Al Mahrūqah Formation in the Murzuq Basin, northern Sahara, Libya evidence for orbitally-forced humid episodes during the last 500,000 years. *Palaeogeogr. Palaeoclimatol. Palaeoecol.* 257, 1–2. doi: 10.1016/j.palaeo.2007.07.001
- Ghezze, E., and Rook, L. (2014). *Cuon alpinus* (Pallas, 1811) (Mammalia, Carnivora) from Equi (Late Pleistocene, Massa-Carrara, Italy): anatomical analysis and palaeoecological contextualisation. *Rend. Lincei* 25, 491–504. doi: 10.1007/s12210-014-0345-6
- Gopalakrishnan, S., Sinding, M.-H. S., Ramos-Madrugal, J., Niemann, J., Samaniego Castruita, J. A., Vieira, F. G., et al. (2018). Interspecific Gene Flow Shaped the Evolution of the Genus *Canis*. *Curr. Biol.* 28, 3441–3449. doi: 10.1016/j.cub.2018.08.041
- Guisan, A., Edwards, T. C., and Hastie, T. (2002). Generalized linear and generalized additive models in studies of species distributions: setting the scene. *Ecol. Modell.* 157, 89–100. doi: 10.1016/S0304-3800(02)00204-1
- Guisan, A., Tingley, R., Baumgartner, J. B., Naujokaitis-Lewis, I., Sutcliffe, P. R., Tulloch, A. I. T., et al. (2013). Predicting species distributions for conservation decisions. *Ecol. Lett.* 16, 1424–1435. doi: 10.1111/ele.12189
- Helmens, K. F. (2014). The last interglacial-glacial cycle (MIS 5-2) re-examined based on long proxy records from central and northern Europe. *Quat. Sci. Rev.* 86, 115–143. doi: 10.1016/j.quascirev.2013.12.012
- Hijmans, R. J., and van Etten, J. (2020). *Raster: Geographic Data Analysis And Modeling*. Available online at: <http://cran.r-project.org/package=raster> (accessed October 26, 2020).
- Johnsingh, A. J. T. (2009). Distribution and status of dhole *Cuon alpinus* Pallas, 1811 in South Asia. *Mammalia* 49, 203–208. doi: 10.1515/mamm.1985.49.2.203
- Jones, K. E., Bielby, J., Cardillo, M., Fritz, S. A., O'Dell, J., Orme, C. D. L., et al. (2009). PanTHERIA: a species-level database of life history, ecology, and geography of extant and recently extinct mammals. *Ecology* 90, 2648. doi: 10.1890/08-1494.1
- Kamler, J., Songsansen, N., Jenks, K., Srivathsa, A., Sheng, L., and Kunkel, K. (2015). *Cuon Alpinus*. *Iucn red list threat. Species 2015 e.t5953a72477893*. Available online at: <https://dx.doi.org/10.2305/IUCN.UK.2015-4.RLTS.T5953A72477893.en> (accessed on Oct 26, 2020).
- Karger, D. N., Conrad, O., Böhrner, J., Kawohl, T., Kreft, H., Soria-Auza, R. W., et al. (2017). Climatologies at high resolution for the earth's land surface areas. *Sci. Data* 4:170122. doi: 10.1038/sdata.2017.122
- Koepfli, K., Pollinger, J., Godinho, R., Stephen, J., Brien, O., Van-Valkenburgh, B., et al. (2015). Genome-wide Evidence Reveals that African and Eurasian Golden Jackals Are Distinct Species. *Curr. Biol.* 25, 2158–2165. doi: 10.1016/j.cub.2015.06.060
- Leite, Y. L. R., Costa, L. P., Loss, A. C., Rocha, R. G., Batalha-Filho, H., Bastos, A. C., et al. (2016). Neotropical forest expansion during the last glacial period challenges refuge hypothesis. *Proc. Natl. Acad. Sci. U. S. A.* 113, 1008–1013. doi: 10.1073/pnas.1513062113
- Leroy, B., Delsol, R., Hugué, B., Meynard, C. N., Barhoumi, C., Barbet-Massin, M., et al. (2018). Without quality presence-absence data, discrimination metrics such as TSS can be misleading measures of model performance. *J. Biogeogr.* 45, 1994–2002. doi: 10.1111/jbi.13402
- Liang, H., Liao, W., Yao, Y., Bae, C. J., and Wang, W. (2020). A late Middle Pleistocene mammalian fauna recovered in northeast Guangxi, southern China: implications for regional biogeography. *Quat. Int.* 563, 29–37. doi: 10.1016/j.quaint.2019.12.013
- Liu, X., Shen, G., Tu, H., Lu, C., and Granger, D. E. (2015). Initial 26Al/10Be burial dating of the hominin site Bailong Cave in Hubei Province, central China. *Quat. Int.* 389, 235–240. doi: 10.1016/j.quaint.2014.10.028
- Makenov, M. (2018). Extinct or extant? A review of dhole (*Cuon alpinus* Pallas, 1811) distribution in the former USSR and modern Russia. *Mamm. Res.* 63, 1–9. doi: 10.1007/s13364-017-0339-8
- Marciszak, A., Kropczyk, A., and Lipecki, G. (2021). The first record of *Cuon alpinus* (Pallas, 1811) from Poland and the possible impact of other large canids on the evolution of the species. *J. Quat. Sci.* 36, 1101–1121. doi: 10.1002/jqs.3340
- Martinez-Freiria, F., Tarroso, P., Rebelo, H., and Brito, J. C. (2016). Contemporary niche contraction affects climate change predictions for elephants and giraffes. *Divers. Distrib.* 22, 432–444. doi: 10.1111/ddi.12406
- Martínez-Navarro, B. (2010). “Early Pleistocene Faunas of Eurasia and Hominin Dispersals,” in *Out Of Africa I: The First Hominin Colonization Of Eurasia*, eds J. G. Fleagle, J. J. Shea, F. E. Grine, A. L. Baden, and R. E. Leakey (Dordrecht: Springer), 207–224. doi: 10.1007/978-90-481-9036-2_13
- Mecozzi, B., Lucenti, S. B., and Iurino, D. A. (2020). *Cuon Alpinus* (Pallas, 1811) From the Late Pleistocene Site of Ingarano (Foggia, Southern Italy) and Insights on the Eurasian Middle To Late Pleistocene Record. *Alp. Mediterr. Quat.* 33, 89–98. doi: 10.26382/AMQ.2020.08
- Middleton, O., Svensson, H., Scharlemann, J. P. W., Faurby, S., and Sandom, C. (2021). CarniDIET 1.0: a database of terrestrial carnivorous mammal diets. *Glob. Ecol. Biogeogr.* 30, 1175–1182. doi: 10.1111/geb.13296
- Nogués-Bravo, D. (2009). Predicting the past distribution of species climatic niches. *Glob. Ecol. Biogeogr.* 18, 521–531. doi: 10.1111/j.1466-8238.2009.00476.x
- Otto-Bliesner, B. L., Marshall, S. J., Overpeck, J. T., Miller, G. H., and Hu, A. (2006). Simulating Arctic Climate Warmth and Icefield Retreat in the Last Interglaciation. *Science* 311, 1751L–1753. doi: 10.1126/science.1120808
- Palkopoulou, E., Lipson, M., Mallick, S., Nielsen, S., Rohland, N., Baleka, S., et al. (2018). A comprehensive genomic history of extinct and living elephants. *Proc. Natl. Acad. Sci. U. S. A.* 115, E2566L–E2574. doi: 10.1073/pnas.1720554115
- Pebesma, E. (2018). Simple Features for R: standardized Support for Spatial Vector Data. *R. J.* 10:439. doi: 10.32614/RJ-2018-009
- Puzachenko, A. Y., and Markova, A. K. (2019). Evolution of mammal species composition and species richness during the Late Pleistocene - Holocene transition in Europe: a general view at the regional scale. *Quat. Int.* 530, 88–106. doi: 10.1016/j.quaint.2018.12.025
- QGIS Development Team (2020). *QGIS Geographic Information System*. QGIS Association. Available online at: <https://www.qgis.org> (accessed October 26, 2020).
- R Core Team (2020). *R: A Language and Environment for Statistical Computing*. Vienna: R Foundation for Statistical Computing.
- Rabosky, D. L., Grundler, M., Anderson, C., Title, P., Shi, J. J., Brown, J. W., et al. (2014). BAMMtools: an R package for the analysis of evolutionary dynamics on phylogenetic trees. *Methods Ecol. Evol.* 5, 701–707. doi: 10.1111/2041-210X.12199
- Ripoll, M. P., Morales Pérez, J. V., Sanchis Serra, A., Aura Tortosa, J. E., and Montañana, I. S. (2010). Presence of the genus *Cuon* in upper Pleistocene and initial Holocene sites of the Iberian Peninsula: new remains identified in archaeological contexts of the Mediterranean region. *J. Archaeol. Sci.* 37, 437–450. doi: 10.1016/j.jas.2009.10.008
- Roucoux, K. H., Tzedakis, P. C., Lawson, I. T., and Margari, V. (2011). Vegetation history of the penultimate glacial period (Marine isotope stage 6) at Ioannina, north-west Greece. *J. Quat. Sci.* 26, 616–626. doi: 10.1002/jqs.1483
- Shao, Q., Bahain, J. J., Wang, W., Zhu, M., Voinchet, P., Lin, M., et al. (2015). Coupled ESR and U-series dating of early Pleistocene *Gigantopithecus* faunas at Mohui and Sanhe Caves, Guangxi, southern China. *Quat. Geochronol.* 30, 524–528. doi: 10.1016/j.quageo.2015.04.008
- Simó-Riudalbas, M., Tarroso, P., Papenfuss, T., Al-Sariri, T., and Carranza, S. (2018). Systematics, biogeography and evolution of *Asaccus gallagheri* (Squamata, Phyllodactylidae) with the description of a new endemic species from Oman. *Syst. Biodivers.* 16, 323–339. doi: 10.1080/14772000.2017.1403496
- Stebbins, G. L. (1959). The Role of Hybridization in Evolution. *Proc. Am. Philos. Soc.* 103, 231–251.
- Stiner, C., Howell, F., and Martínez-Navarro, B. (2001). Outside Africa: middle Pleistocene *Lycaon* from Hayonim Cave, Israel. *Boll. Della Soc. Paleontol. Ital.* 40, 293–302.

- Stiner, M. C., Arsebük, G., and Howell, F. C. (1996). Cave bears and paleolithic artifacts in Yarimburgaz Cave, Turkey: dissecting a palimpsest. *Geoarchaeology* 11, 279–327.
- Taron, U. H., Paijmans, J. L. A., Barlow, A., Preick, M., Iyengar, A., Drăgușin, V., et al. (2021). Ancient DNA from the asiatic wild dog (*Cuon alpinus*) from Europe. *Genes* 12:144. doi: 10.3390/genes12020144
- Taylor, S. A., and Larson, E. L. (2019). Insights from genomes into the evolutionary importance and prevalence of hybridization in nature. *Nat. Ecol. Evol.* 3, 170–177. doi: 10.1038/s41559-018-0777-y
- Thuiller, W., Lafourcade, B., Engler, R., and Araújo, M. B. (2009). BIOMOD – a platform for ensemble forecasting of species distributions. *Ecography* 32, 369–373. doi: 10.1111/j.1600-0587.2008.05742.x
- Tzedakis, P. C., Roucoux, K. H., de Abreu, L., and Shackleton, N. J. (2004). The duration of forest stages in southern Europe and interglacial climate variability. *Science* 306, 2231–2235. doi: 10.1126/science.1102398
- Varela, S., Anderson, R. P., García-Valdés, R., and Fernández-González, F. (2014). Environmental filters reduce the effects of sampling bias and improve predictions of ecological niche models. *Ecography* 37, 1084–1091. doi: 10.1111/j.1600-0587.2013.00441.x
- Varela, S., Rodríguez, J., and Lobo, J. M. (2009). Is current climatic equilibrium a guarantee for the transferability of distribution model predictions? A case study of the spotted hyena. *J. Biogeogr.* 36, 1645–1655. doi: 10.1111/j.1365-2699.2009.02125.x
- Vieira, E. M., and Port, D. (2007). Niche overlap and resource partitioning between two sympatric fox species in southern Brazil. *J. Zool.* 272, 57–63. doi: 10.1111/j.1469-7998.2006.00237.x
- Volmer, R., van der Geer, A. A. E., Cabrera, P. A., Wibowo, U. P., and Kurniawan, I. (2019). When did *Cuon* reach Java? – Reinvestigation of canid fossils from *Homo erectus* faunas. *Geobios* 55, 89–102. doi: 10.1016/j.geobios.2019.06.004
- Warren, D. L., Glor, R. E., and Turelli, M. (2008). Environmental niche equivalency versus conservatism: quantitative approaches to niche evolution. *Evolution* 62, 2868–2883. doi: 10.1111/j.1558-5646.2008.00482.x
- Westbury, M. V., Hartmann, S., Barlow, A., Preick, M., Ridush, B., Nagel, D., et al. (2020). Hyena paleogenomes reveal a complex evolutionary history of cross-continental gene flow between spotted and cave hyena. *Sci. Adv.* 6, eaay0456. doi: 10.1126/sciadv.aay0456
- Willis, P. M. (2013). Why do animals hybridize? *Acta Ethol.* 16, 127–134. doi: 10.1007/s10211-013-0144-6
- Wilman, H., Belmaker, J., Simpson, J., de la Rosa, C., Rivadeneira, M. M., and Jetz, W. (2014). EltonTraits 1.0: species-level foraging attributes of the world's birds and mammals. *Ecology* 95:2027. doi: 10.1890/13-1917.1
- Woodroffe, R., Ginsberg, J., Macdonald, D. W., and Iucn/Scs Canid Specialist Group. (1997). *The African Wild Dog - Status Survey And Conservation Action Plan*. Gland: IUCN.
- Woodroffe, R., and Sillero-Zubiri, C. (2020). *Lycaon Pictus*. *Iucn red list threat. Species 2020 e.t12436a166502262*. Available online at: <https://dx.doi.org/10.2305/IUCN.UK.2020-1.RLTS.T12436A166502262.en> (accessed on Oct 26, 2020).

Conflict of Interest: The authors declare that the research was conducted in the absence of any commercial or financial relationships that could be construed as a potential conflict of interest.

Publisher's Note: All claims expressed in this article are solely those of the authors and do not necessarily represent those of their affiliated organizations, or those of the publisher, the editors and the reviewers. Any product that may be evaluated in this article, or claim that may be made by its manufacturer, is not guaranteed or endorsed by the publisher.

Copyright © 2022 Rocha, Gonçalves, Tarroso, Monterroso and Godinho. This is an open-access article distributed under the terms of the Creative Commons Attribution License (CC BY). The use, distribution or reproduction in other forums is permitted, provided the original author(s) and the copyright owner(s) are credited and that the original publication in this journal is cited, in accordance with accepted academic practice. No use, distribution or reproduction is permitted which does not comply with these terms.